M. A. Garces[1], M. Colet[1], B. Williams[1]

[1]Infrasound Laboratory, University of Hawaii, Manoa.

Corresponding author: Milton Garces (milton@isla.hawaii.edu)

ORCID: https://orcid.org/0000-0002-2768-3812

Submitted: 2022-10-21

Data URL Updated: 2022-10-27

Key Points:

- High-quality pressure, wind, and temperature data sampled once a minute are available from a weather station Nuku alofa (NUKU) in Tonga managed by the Australian Bureau of Meteorology and supported by the Tongan Meteorological Services.
- The NUKU barometer, at a range of 68 km, recorded a depressurization during the climactic stage of the 2022 Tonga eruption and the radiation of Lamb waves.
- However, the Lamb waves were observed as propagating overpressure pulses by stations at ranges of 700 km or greater.
- The near-source depressurization could be explained by flow around a Rankine half-body.
- The NUKU data could be part of the validation stage of more sophisticated fluid dynamic models of eruption source processes.

Abstract

A weather station in Nuku alofa (NUKU), Tonga, ~68km away from the epicenter of the 2022 Tonga eruption, recorded exceptional pressure, temperature, and wind data representative of the eruption source hydrodynamics. These extraordinary high-quality data are available for further source and propagation studies. In contrast to other barometers and infrasound sensors at greater ranges, the NUKU barometer recorded a decrease in pressure during the climactic stage of the eruption. A simple fluid dynamic explanation of the depressurization is provided, with a commentary on near- vs far-field pressure observations of very large eruptions.

Plain Language Summary

The primary Lamb wave of the 2022 Tonga eruption was recorded as a pressure drop of ~18 hPa from ambient at the NUKU barometer, ~68 km from the source. It may be interpreted, to first order, by the proximity of the station to a Rankine half-body sustained by the prevailing winds and the flow induced by the volcanic source.

1 Introduction

The corpus of literature on acoustic-gravity waves radiated during the 2022 Tonga eruption [e.g. Matoza et al. (2022), Vergoz et al. (2022)] will undoubtedly grow rapidly in the next years. The interpretation of rarely encountered oscillation modes at smaller acoustic and larger planetary (e.g. Watada et al. 2022) scales rely on source models derived from validated observations. This paper concentrates on a key meteorological station in Tonga, the near field of the Lamb wave, that can serve as verification data for future source models.

The Nuku alofa (NUKU) barometer station in Tonga is at a range of ~68 km in a direction SSE from the volcano's epicenter (Figure 1). NUKU observed a depressurization associated with the Lamb wave radiation, in contrast to the compression (pressurization) observed at other barometers and IMS infrasound stations throughout Earth. The observed pressure drop may be attributed to near-field hydrodynamic effects.

In wave propagation, the near field and the far field are defined relative to the wavelength of a source. Stations distances within a wavelength are considered to be in the near field, where hydrodynamic conditions dominate, and a fluid is often treated as incompressible. However, at large station distances greater than a wavelength, the radiated wavefield is the average over the source region and the atmosphere (at the time scales of the Lamb wave) is treated as a compressible fluid under the influence of gravity. The nominal dominant period of the primary Lamb wave of ~2000 s (e.g. Vergoz et al., 2022) corresponds to a wavelength of ~600 km. The upper bound for the explosive TNT yield equivalent of the primary Lamb wave was ~200 megatonnes (Vergoz et al., 2022; Adushkin et al. 2022), consistent with its Volcano Explosivity Index (VEI) 6 estimate. The 2022 Tonga eruption produced the most powerful blast on Earth since the 1883 Krakatau eruption (e.g. Matoza et al., 2022). The NUKU station was within ~1/10 of a wavelength, and well within the near field.

2 Barometer and Wind Data

The NUKU barometer is a Vaisala PTB220B, and the wind sensor is a RM Young 05103 Anemometer. The NUKU station is at a range of ~68 km from the source and was presented in Vergoz et al (2022), Figure 4. The next closest barometer with openly available, validated data is in Maopo'opo, Futuna (FUTU), at a range of ~744 km (Vergoz et al. 2022, Figure 7). As noted in GVP (2022), Matoza et al. (2022), and Vergoz et al. (2022), substantial eruptive activity took place during 14 January. Note the GVP report uses local time, UTC + 13. Eruptive activity in 15 January for the climactic 15 January episode was underway by ~4:00 UTC (17:00 local time) and escalated into major explosions at 04:15. The second sequence began around 08:26, with a massive eruption at 08:31 that radiated the secondary Lamb wave. It is important to note that the new thermodynamic and flow conditions could be considered as initialized at ~04:00 UTC, and in conjunction with the 14 January activity, the atmosphere was primed to respond to a change in fluid flux.

The barometer pressure, wind bearing direction, and wind speed data at NUKU

are shown in Figure 1, where the time scale is in hours relative to the nominal main event time of 04:15 UTC on 15 January 2022. The large pressure excursion at the NUKU barometer (Figure 1a) shortly after the 0 hour corresponds to the travel time for a Lamb wave propagating at ~310 m/s. The second Lamb wave shown in Vergoz et al. (2022), Figure 4, arrives at NUKU ~4:15 after the main event, also with a pressure drop in its largest excursion. The NUKU pressure waveforms are similar to other barometers with ranges greater than the nominal 600 km wavelength (Vergoz et al. (2022), Figure 7), but is reversed in sign. The maximum pressure drop of ~18 hPa in the NUKU barometer is associated with the primary Lamb wave, with substantial fluctuations in the wind speed and direction (Figure 1).

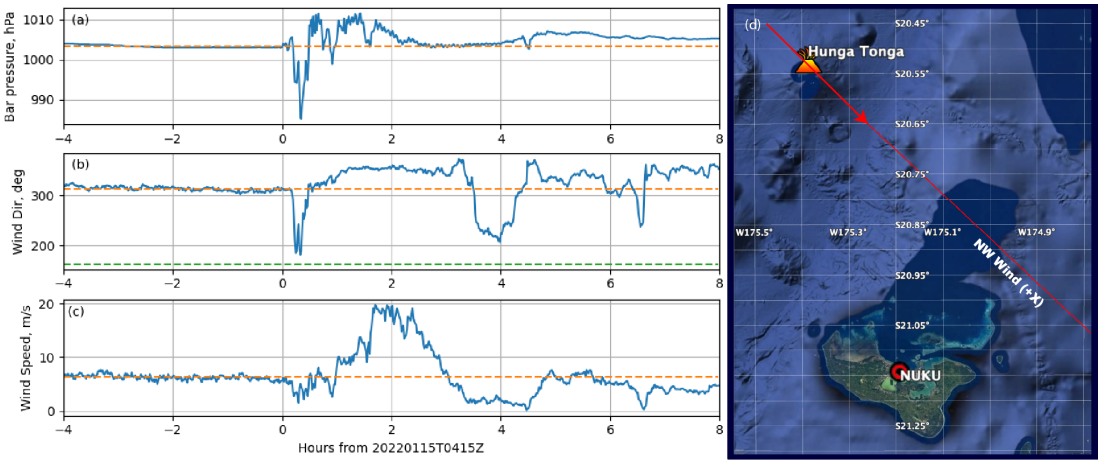

Figure 1. (a) Pressure in hPa, (b) wind bearing in degrees relative to N, and (c) wind speed in m/s. The map (d) shows the relative orientation of the source, station, and the initial wind conditions. The initial wind direction is used as the positive horizontal (x) axis for the Rankine body in Figure 2. The dashed orange line is the average over the first four hours (before the zero hour) and the green line is the angle towards the volcano.

The pressure records are initially puzzling, as they show a pressure drop associated with a large transient mass flux that appeared to substantially alter the recorded wind speed and direction. In the context of global circulation patterns, the Tonga event is a brief and highly localized perturbation in time and space. The ambient winds are the generally the result of thermal and rotational forces at much greater scales than the eruption transient. However, if we consider the wind field preceding the eruption as a free stream, the volcanic event as a source flow, and the station as a measurement point within the near-field hydrodynamic regime, it is possible to explain some of the pressure observations, to first order, in terms of the familiar Rankine half-body flow. This interpretation is a coarse simplification of a complicated problem; however, it can be used as a first-order explanation and a benchmark for more sophisticated models.

3 Near-field Hydrodynamic Interpretation

As previously noted, starting ~04:00 UTC the atmosphere is primed for a change in the flow regime. The arrival of the primary Lamb wave carries the information to the station that the flux rate has changed. We postulate that the new mass flux can support a transitory Rankine body that reverses the sign of the gauge pressure and persists for the ~30 minute period of the Lamb wave. After the paroxysmal eruption stage, the thermodynamic state of the atmosphere is likely to be substantially altered, the steady free stream initial conditions are no longer valid, and a new flow regime should be considered. This section to provide a plausible explanation for the observed depressurization at the NUKU station during the passage of the Tonga Lamb wave in the near field. The time scale of the Lamb wave perturbation is short relative to planetary scales, long relative to acoustic scales. To first order, the fluid near the source is treated as an incompressible, inviscid, irrotational fluid and we consider flow along a hypothetical streamline near the ground surface.

The velocity potential solution for the superposition of a free stream and a source flow (e.g. Barba and Mesnard, 2019) can be expressed as

$\varphi = Ux + \frac{m}{2\pi}\ln(r)$,

with resulting vector velocity field

$\overrightarrow{V} = \nabla\varphi = U\hat{1}_x + \frac{m}{2\pi r}\hat{1}_r$,

where U is the free stream speed, in this case the speed of the trade winds, which defines the positive x horizontal axis, and r is the radial distance from the source with planar mass flux m. This superposition is well known, and creates a fluid flow known as the Rankine half-body. It has a well-defined stagnation point where the stream and radial velocity match, and a dividing streamline that clearly separates the flow regimes (Figure 2).

The pressure can be recovered from Bernoulli's hydrodynamic equation along a streamline

$P_U + \frac{\rho U^2}{2} = P_V + \frac{\rho V^2}{2}$,

where P_U is the pressure in the free stream far from the source, and P_V is the pressure where the velocity is measured closer to the source. The pressure variability is efficiently expressed by the pressure coefficient C_P

$C_P = \frac{P_V - P_U}{\frac{1}{2}\rho U^2} = 1 - \left(\frac{V}{U}\right)^2$.

In a still atmosphere ($\mathbf{U} = \mathbf{0}$), a sustained peak pressure differential of ~18 hPa and a nominal atmospheric density of ~1 kg/m^3 would produce an exceedingly strong gust speed of $\mathbf{V \approx 60\ \frac{m}{s} \approx 117\ knots}$ at some height above the no-slip ground surface where boundary layer and obstructions would have a minimal effect. However, such strong wind speeds are not observed at the NUKU station. We average over the first four hours of the record shown in Figure 1 to

estimate a free stream pressure of $\mathbf{P_U}$=1003.25 hPa, a wind bearing of 313.24 degrees relative to North, and mean wind speed of U=6.3 m/s. The stream direction is selected as the horizontal axis (x) in Figure 2. Although all the flow computations were made using MKS/Pa units, the final results in Figure 2 are scaled back to distance in km.

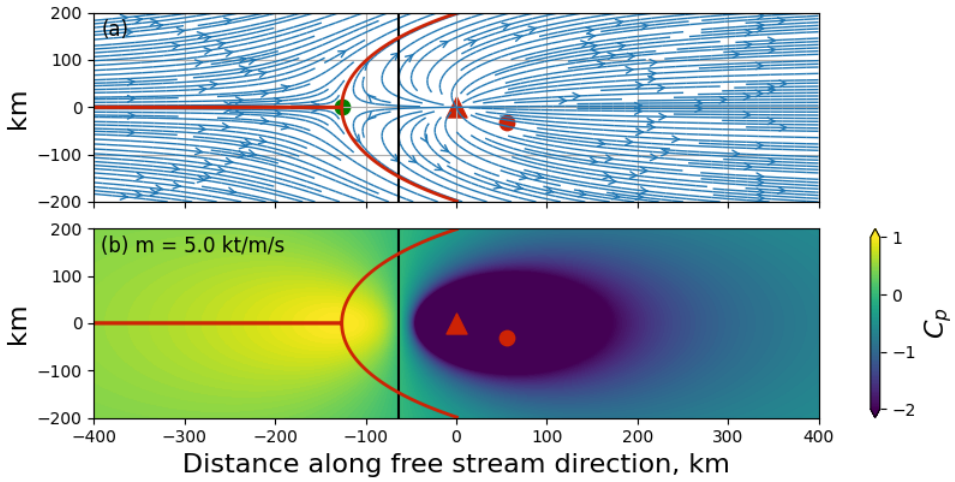

Figure 2. (a) Velocity streamlines and (b) Bernoulli pressure for a Rankine half-body for a source (red triangle) aligned with the direction of the free stream. The red line denotes the dividing streamline, the green dot in (a) is the stagnation point where the free stream speed matches the source flow speed. The source is placed at x, y = (0, 0). The black line marks the pressure equilibration boundary; to the left of the line, $C_P > 0$ and the observed pressure will be greater than the ambient pressure. A measurement station to the right of the black line will observe a pressure drop relative to ambient. The location on NUKU relative to the source is represented as a red dot.

A pressure equilibration boundary can be derived where $\mathbf{P_V}-\mathbf{P_U}=\mathbf{0}$, $\mathbf{C_P}=\mathbf{0}$. This corresponds to the line

$$\mathbf{x} = -\frac{\mathbf{m}}{\mathbf{4\,U}}.$$

The Rankine flow computed for a source with a mass flux m=5x10^6 kg/m/s=5 kilotonnes/m/s is shown in Figure 2. Although this is a large number, it is well within the range of the equivalent 200 megatonne yield of the Tonga Lamb wave. For this source flow regime, the NUKU station will be to the right of the black equilibration line and therefore the pressure excursion would be negative. To first order, the observed near-field negative pressure for a positive mass flux could be interpreted as the result of the station positioned in the negative pressure region of the Rankine body.

The flow field computed for a sink with a mass flux m=-5x10^6 kg/m/s=-5 kilotonnes/m/s is shown in Figure 3. The NUKU station will still be positioned in

the negative pressure region of the Rankine body for this sink and free stream flow regime. This would correspond to a substantial updraft, or drawing of fluid away from the station during the eruption. In some ways, the predicted wind flow for the sink model better matches the observed wind field, which points towards the volcano around the time of the Lamb wave arrival. This sink term is consistent with the elevated heat source of Watada et al. (2022), which also predicts a negative pressure within 150km of the source.

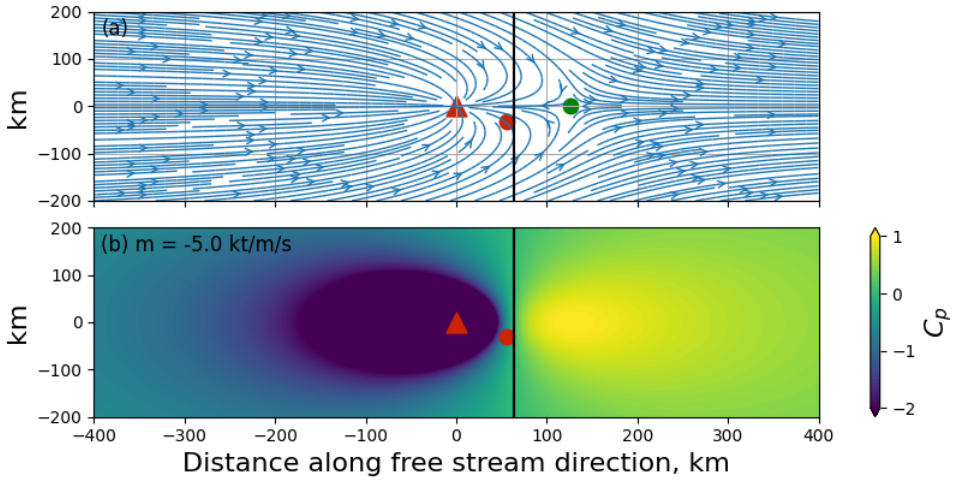

Figure 3. (a) Velocity streamlines and (b) Bernoulli pressure for a Rankine half-body for a sink (red triangle) aligned with the direction of the free stream. The flow sink is placed at x, y = (0, 0). The black line marks the pressure equilibration boundary; to the right of the line, $C_P > 0$ and the observed pressure will be greater than the ambient pressure. A measurement station to the left of the black line will observe a pressure drop relative to ambient. The location on NUKU relative to the source is represented as a red dot.

Despite its coarse simplicity, the potential flow interpretation is surprisingly robust; whether the eruption is acting as a mass source or a sink, or the free stream direction were to be reversed (heading vs bearing), the station would still be within the depressurized region of the Rankine body for a mass flux of ~5kt/m/s. Increasing the mass flux would increase the scale of the Rankine body, enhancing the depressurization. Although this simple model cannot explain all the observed features, it can help interpret the observed pressure drop at NUKU for diverse flow regimes.

5 Conclusion

The pressure drop observed by the Nuku'alofa (NUKU barometer during the arrival of the Tonga Lamb wave can be interpreted, to first order, by a Rankine half-body in the near-field hydrodynamic range of the source. The extraordinary high-quality met data collected at NUKU is available for further studies. More sophisticated hydrodynamic source models, coupled with higher-order planetary

(e.g. Watanabe et al. 2022) and acoustic gravity wave models will be able to shed a brighter light on the eruption chronology and energergy. Our study highlights some of the differences between near and far field pressure fields, and reinforces the notion that this volcanic eruption did not behave like a detonation during the emission of the Tonga Lamb wave (e.g. Vergoz et al. 2022), which would present as an overpressure in the near as well as the far field.

Acknowledgments

There are no conflicts of interest. The data were made available by R. Greenwood, J. Aquilina, and J. Chittleborough with the Climate & Oceans Support Program in the Pacific (COSPPac), an Australian Aid project managed by the Australian Bureau of Meteorology and supported by the Tongan Meteorological Services; this paper would not have been possible without them. Many thanks to J. Vergoz, B. Taisne, R. Matoza, and D. Fee for pointing the way.

Funding: This paper was supported by the Department of Energy National Nuclear Security Administration under Award Numbers DE-NA0003920 (MTV) and DE-NA0003921 (ETI).

Data Availability Statement: The raw NUKU data is available from the Australian Bureau of Meteorology upon request. The raw data were loaded as Pandas data frames and converted to MKS units. The curated NUKU barometer, wind, and temperature data used in this study are presently available as pickled Panda data frames at:

https://www.higp.hawaii.edu/archive/isla/Tonga_220115/NUKU/

This is only temporary data access point for the purposes of the paper review while we set up a longer-term distribution point at the University of Hawaii. The flow fields in Figures 2 and 3 were produced using the methods of Barba and Mesnard (2019).

References

Adushkin, V.V., Rybnov, Yu.S., Spivak, A.A. (2022). Geophysical Effects of the Eruption of Hunga–Tonga–Hunga–Ha'apai Volcano on January 15, 2022. Dokl. Earth Sc. 504, 362–367. https://doi.org/10.1134/S1028334X22060034

Barba, Lorena A., and Mesnard, Olivier (2019). Aero Python: classical aerodynamics of potential flow using Python. Journal of Open Source Education, 2(15), 45, https://doi.org/10.21105/jose.00045

Global Volcanism Program, 2022. Hunga Tonga-Hunga Ha'apai (Tonga) Surtseyan explosions with eruption plumes during 14-15 January 2022. Report on Hunga Tonga-Hunga Ha'apai (Tonga) (Bennis, K.L., and Venzke, E., eds.). Bulletin of the Global Volcanism Network, 47:3 (March 2022). Smithsonian Institution, https://volcano.si.edu/showreport.cfm?doi=10.5479/si.GVP.BGVN202203-243040

Matoza, R.S., Fee, D., Assink, J.D., Iezzi, A.M., Green, D.N., et al. (2022). Atmospheric waves and global seismoacoustic observations of the January 2022 Hunga eruption, Tonga. Science 377, 95–100. https://doi.org/10.1126/science.abo7063

Vergoz, J., Hupe, P., Listowski, C., Le Pichon, A., Garcés, M.A., et al. (2022). IMS observations of infrasound and acoustic-gravity waves produced by the January 2022 volcanic eruption of Hunga, Tonga: A global analysis. Earth and Planetary Science Letters 591, 117639. https://doi.org/10.1016/j.epsl.2022.117639

Watanabe, S., Hamilton, K., Sakazaki, T., Nakano, M., 2022. First Detection of the Pekeris Internal Global Atmospheric Resonance: Evidence from the 2022 Tonga Eruption and from Global Reanalysis Data. Journal of the Atmospheric Sciences. https://doi.org/10.1175/JAS-D-22-0078.1